JOURNAL OF SOLID STATE CHEMISTRY, 31, 233–247 (1980)

Theory and Practice of a Powerful Technique for Electrochemical Investigation of Solid Solution Electrode Materials

G. J. DUDLEY†* AND B. C. H. STEELE

Wolfson Unit for Solid-State Ionics, Department of Metallurgy and Materials Science, Imperial College of Science and Technology, London SW7 2AZ, United Kingdom

Received February 6, 1979

The theory and practice of a solid-state electrochemical technique which allows measurement of the chemical diffusion coefficient and partial conductivities of the mobile species in a mixed ionic–electronic conductor, as well as the equilibrium partial thermodynamic quantities, are described. The theory incorporates nonideal thermodynamic behavior of the carriers as well as cross terms in the flux equations. Once the cell is assembled, all parameters can be measured as a function of composition without any further physical manipulation, so that the experiments are well suited to automatic control.

1. Introduction

With the successful development of solid electrolyte materials in recent years more emphasis in the field of solid-state electrochemistry is being directed toward the study of superionic conductors which are also good electronic conductors, have a wide range of stoichiometry for the mobile ion, and are thus of interest for use in batteries. These solid solution electrode (SSE) materials have been discussed in detail by Steele (*1*), Armand (*2*), and Whittingham (*3*).

The most important parameters of SSEs for battery applications are the range of stoichiometry; the activity of the mobile ion as a function of composition, which governs the change in open-circuit emf of a cell during charge–discharge cycles; and the chemical or ambipolar diffusion coefficient $\tilde{D}$, which places an upper limit on the current density obtainable from a given cell geometry.

In order to better understand the materials, however, it is also desirable to be able to measure separately the two conductivities and their activation energies, while determinations of the partial entropy and enthalpy from the temperature variation of the cell emf can give useful information about the distribution of ions among sites of different energies (*2, 4, 5*).

Alternating current conductivity has become the most widely used method for investigating the ionic conductivity of electrolytes. In the case of mixed ionic–electronic conductors, however, the ac technique yields only the total conductivity and dc measurements are normally required to identify the contributions of the different carriers to the total conductivity. Widely used dc techniques include the cell emf, Hebb–Wagner,

* To whom correspondence should be addressed.

† Present address: Berec Group Ltd., Advanced Projects Group, 18, Nuffield Way, Ashville Trading Estate, Abingdon, Oxon OX14 1TG, United Kingdom.

0022-4596/80/020233-15$02.00/0

and Tubandt electrolysis arrangements, while for predominantly electronic conductors pulse and galvanostatic methods are applicable, the ionic conductivity following from the measured chemical diffusion coefficient and a thermodynamic factor. These techniques have been reviewed by Wagner (*6*), and very recently by Weppner and Huggins (*7*). The technique described in this work, also mentioned in the above reviews, has been used considerably in studies of silver and copper chalcogenides, for example, by Miyatani (*8–10*), Rickert (*11*), Takahashi and Yamamoto (*12*), and recently by Dudley *et al.* for ternary potassium, lithium, and copper ion mixed conductors (*4, 5, 13, 14*).

Although the main theoretical aspects of the technique have been treated by Yokota (*15, 16*) and Wagner (*6,17*) the present authors feel that all its potential have not been widely recognized, let alone exploited, and that it has much to offer as a precise technique for measuring the transport properties of recently developed solid solution electrode materials. In this paper we have attempted to produce a completely general treatment of the technique, drawing on the ideas of Kimball (*18*), Wagner, and Yokota but extending and generalizing where possible. It is shown, for instance, that both cross terms in the flux equations and thermodynamic nonideality can be incorporated without great difficulty. In Section 2 we briefly describe the cell configurations used and the significance of the various probe voltages, while in Section 3 we cover first the theory of steady-state conditions and then describe time-dependent behavior. In the remaining sections the more practical aspects of the technique are covered.

2. Principle of the Method

Just as the errors due to nonohmic current contacts or contact resistance can be eliminated in electronic conductivity measurements by the use of two additional voltage probes situated at a known distance apart on the sample, so the same principle can be employed in the case of ionic conductors. The reason for the greater accuracy of four-point techniques can be seen from the equivalent circuit in Fig. 1a, where contact resistances are indicated by R_c and R_p. R_c introduces errors in two-point measurements because the current flowing through produces a voltage drop between contacts and sample. On the other hand R_p, although usually larger than R_c, has no effect provided the voltage-measuring device draws negligible current. The ordinary electronic four-point arrangement is shown in Fig. 1b. In the ionic case a means of converting an external electronic current into an ionic one is

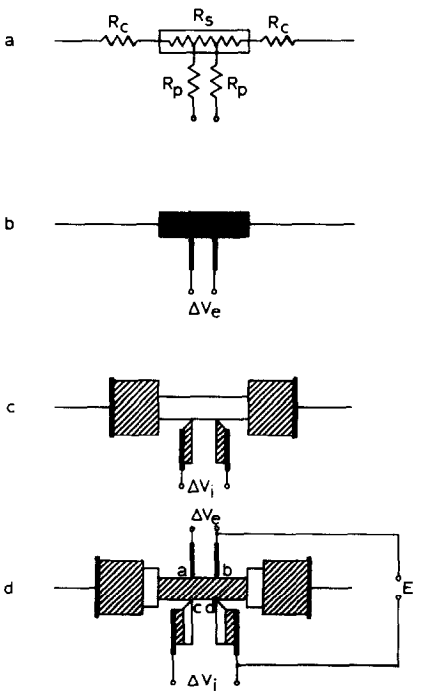

FIG. 1. Types of four-point conductivity experiments. (a) Equivalent circuit showing contact resistances. (b) Electronic four-point arrangement. (c) Ionic four-point arrangement for electrolyte sample. (d) Ionic four-point arrangement for mixed conductor including both ionic and electronic probes.

required. Consider first a sample which is only ionically conducting (electrolyte). The ionic current can be provided by pieces of a mixed conductor which will be referred to as "reservoirs" and which conduct the same ions as the sample as well as electrons, as shown in Fig. 1c. The ionic voltage probes are made from similar mixed-conductor material. In this case, however, equilibrium between the sample and probes is not perturbed by a net current and the electrochemical potential of the ions, μ_{M^+}, in the sample adjacent to a probe is the same as that within the mixed conducting probe itself. Within the latter the electrochemical potential of the ions is related to that of the electrons by equilibria such as

$$M^+ + e^- \rightleftharpoons M.$$

In terms of chemical potentials, this gives

$$\mu_{M^+} + \mu_{e^-} = \mu_M. \qquad (2.1)$$

which because of the equal and opposite charges of M^+ and e^- is the same as

$$\bar{\mu}_{M^+} + \bar{\mu}_{e^-} = \mu_M, \qquad (2.2)$$

where the bars indicate electrochemical potentials. While no net charge is transferred between sample and probe, μ_M remains constant.

A difference in electrochemical potential of ions in the bar between the probes therefore produces an equal but opposite difference in electrochemical potential of electrons in the probes themselves and the voltage difference ΔV_i measured between the ionic probes is given simply by

$$\Delta V_i = -\Delta\bar{\mu}_e/F = +\Delta\bar{\mu}_{M^+}/F. \qquad (2.3)$$

Such experiments have been carried out, for example, on β-alumina (*19*) and $Li_{14}ZnGe_4O_{16}$ (*20*). Next consider a sample which is a mixed conductor. It is necessary to know whether the current flowing through is electronic or ionic. In the first case the ordinary electronic four-point arrangement can be used, employing inert metal contacts at the ends of the sample which are blocking to ions. The second case requires slices of electrolyte between sample and reservoirs to block passage of electrons or holes, as shown in Fig. 1d. Two types of voltage probes can now be distinguished, and their responses derived from considering the free-energy change involved in the hypothetical case of transferring 1 Faraday of charge from one probe to the other.

Electronic probes are made from an inert electronic conductor and are blocking to ions so that

$$\Delta V_e = -(1/F)((\bar{\mu}_e)_b - (\bar{\mu}_e)_a). \qquad (2.4)$$

Ionic probes, in order to be blocking to electrons, now must consist of an electrolyte in contact with the bar and a mixed conductor "reference" material in contact with the electrolyte. Therefore,

$$\Delta V_i = -(1/F)((\bar{\mu}_i)_d - (\bar{\mu}_i)_c). \qquad (2.5)$$

An additional important *cell voltage* (E) is defined between ionic and electronic probes when the bar is in equilibrium. It can be seen that

$$E = -\frac{1}{F}\{(\bar{\mu}_e)_b + (\bar{\mu}_i)_d - (\mu_M)_{\text{ref}}\} \qquad (2.6)$$

$$= -\frac{1}{F}\{(\mu_M)_{\text{sample}} - (\mu_M)_{\text{ref}}\}. \qquad (2.7)$$

The second expression shows that E is the emf of a concentration cell in metal M and if $\mu_{M\,\text{ref}}$ is known the formal activity of metal in the sample is obtained. (This is equivalent to the "atomic probe" described by Ohachi and Taniguchi (*21*).) Changes in E correspond to the open circuit voltage variations expected if the sample material were to be used as a battery electrode. A further important difference occurs when the sample is a mixed conductor. For solely electronic or ionically conducting samples when the current is switched on the voltage probes respond immediately giving a steady voltage. In the mixed-conductor case this is not so; both

types of probes give voltages that change with time, eventually reaching a steady state. As will be shown later this is due to a diffusion process.

3. Phenomenological Theory of Transport in Mixed Conductors

(a) Initial and Steady-State Conditions

We consider a typical solid solution electrode material where there is one mobile ionic species and electrons or holes (i.e., one type completely dominant), moving through a lattice which is fixed as the frame of reference. Considering these three constituents the usual flux equations for one-dimensional transport along the z axis can be written, including cross terms, as

$$J_1 = L_{11}\, d\bar{\mu}_1/dz + L_{12}\, d\bar{\mu}_2/dz + L_{13}\, d\bar{\mu}_3/dz, \quad (3.1)$$

$$J_2 = L_{21}\, d\bar{\mu}_1/dz + L_{22}\, d\bar{\mu}_2/dz + L_{23}\, d\bar{\mu}_3/dz, \quad (3.2)$$

$$J_3 = L_{31}\, d\bar{\mu}_1/dz + L_{32}\, d\bar{\mu}_2/dz + L_{33}\, d\bar{\mu}_3/dz. \quad (3.3)$$

Each molar flux is thus assumed to be linearly proportional to the gradients of chemical potential via the Onsager L coefficients. Species 3 will be identified with the "framework" part of the structure, and to make it the reference frame requires $J_3 = 0$ (Eq. (3.3)). The electrochemical potential gradients of the three species are also related by the Gibbs–Duhem equation giving (*22*)

$$c_1\, d\bar{\mu}_1/dz + c_2\, d\bar{\mu}_2/dz + c_3\, d\bar{\mu}_3/dz = 0. \quad (3.4)$$

Combining Eqs. (3.3) and (3.4), one obtains

$$(L_{31} - c_1 L_{33}/c_3)\, d\bar{\mu}_1/dz + (L_{32} - c_2 L_{33}/c_3)\, d\bar{\mu}_2/dz = 0. \quad (3.5)$$

Table I shows some examples of how actual mixed conductors might be treated.

TABLE I

Compound	Species 1	Species 2	Species 3
$K_{1+x}Fe_{11}O_{17}$	$(1+x)K^+$	xe^-	$(Fe_{11}O_{17})^-$
$Ag_{2-x}Te$	$(2-x)\,Ag^+$	xh^+	Te^{2-}
Li_xTiS_2	xLi^+	$(x+n)e^-$	$(TiS_2)^{n+}$

Species 1, 2, and 3 are not thermodynamic components of the systems in the normal phase rule sense; in fact the examples are binary or pseudobinary. However, the flux equations are valid not only for conditions of local charge neutrality but also where space charges are present. If the requirement of local charge neutrality is not considered, therefore, the three species can be regarded as components and the assumption can be made that any two of the three electrochemical potential gradients can be regarded as independent. Each of the terms in brackets in (3.5) must therefore be equal to zero. Moreover, it is also reasonable to assume that L_{33} is zero since it contains the absolute mobility of the framework. The cross terms L_{31} and L_{32} are thus zero and, with the Onsager reciprocal relations applied, the flux equations reduce to the usual form for two mobile species (*17*):

$$J_1 = L_{11}\, d\bar{\mu}_1/dz + L_{12}\, d\bar{\mu}_2/dz, \quad (3.6)$$

$$J_2 = L_{12}\, d\bar{\mu}_1/dz + L_{22}\, d\bar{\mu}_2/dz. \quad (3.7)$$

It is important to point out, however that Eqs. (3.6) and (3.7) are now already compatible with the Gibbs–Duhem equation, yet no restrictions relating $d\bar{\mu}_1/dz$ and $d\bar{\mu}_2/dz$ have resulted. If, on the other hand, the framework is not considered and the Gibbs–Helmholtz equation is combined with just the flux equations pertaining to mobile species (i.e., Eqs. (3.6) and (3.7)) inconsistencies result except in the case of zero fluxes (*22*).

In the flux equations we have not explicitly included other species which may be present,

such as metal atoms arising from the equilibrium:

$$M^+ + e^- \rightleftharpoons M.$$

Such effects can be regarded as extreme cases of interactions between species which are allowed for by nonzero cross coefficients and the thermodynamic factors (to be considered later).

The L coefficients are defined by (17)

$$L_{ij} = -c_i B_{ij}. \tag{3.8}$$

The electrochemical potential gradients can be split up into their chemical and electrostatic components:

$$d\bar{\mu}_i/dz = d\mu_i/dz + z_1 F\, d\varphi/dz. \tag{3.9}$$

φ is the local electrostatic potential averaged over a region of space which is large compared to atomic dimensions, but small compared to the dimensions of the sample, as discussed by Wagner (*17*). Conductivity coefficients σ_{ij} can then be defined as

$$\sigma_{ij} = -L_{ij} z_i z_j F^2 \tag{3.10}$$

and the flux equations can thus be rewritten

$$J_1 = -\frac{\sigma_{11}}{z_1^2 F^2}\left(\frac{d\mu_1}{dz} + z_1 F_1 \frac{d\varphi}{dz}\right) - \frac{\sigma_{12}}{z, z_2 F^2}\left(\frac{d\mu_2}{dz} + z_2 F \frac{d\varphi}{dz}\right), \tag{3.11}$$

$$J_2 = -\frac{\sigma_{12}}{z_1 z_2 F^2}\left(\frac{d\mu_1}{dz} + z_1 F \frac{d\varphi}{dz}\right) - \frac{\sigma_{22}}{z_2^2 F^2}\left(\frac{d\mu_2}{dz} + z_2 F \frac{d\varphi}{dz}\right). \tag{3.12}$$

These are to be preferred since simple combinations of σ_{ij} are experimentally measurable quantities. We will now show how this comes about by reference to eight-point bar conductivity experiments. The relations are the same as those derived by Kimball (*18*) and Wagner (*17*).

Figure 2 shows the characteristic response of ionic and electronic voltage probes during a typical experiment. Before the current is switched on the sample is at equilibrium and within the bar (except at the surfaces) no gradients of chemical potential exist. At t_0, a constant current I_1 of species 1 is switched on. Both species 1 and 2 begin to migrate in the electric field and before any chemical potential gradients have had time to be set up one obtains from Eqs. (3.11) and (3.12)

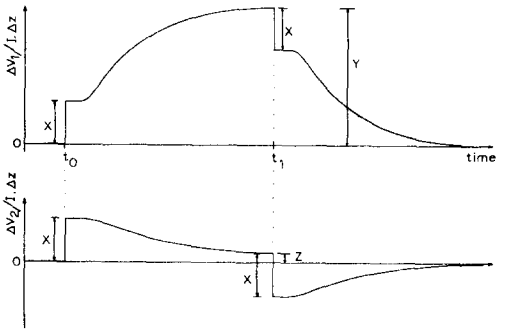

FIG. 2. Behavior of voltage probes reversible to species 1 and 2 on switching on and off a current of species 1. The current is on at t_0 and off at t_1.

$$I_1 = z_1 F J_1 + z_2 F J_2 = -(\sigma_{11} + \sigma_{22} + 2\sigma_{12})\, d\varphi/dz. \tag{3.13}$$

The effective conductivity is thus the total conductivity, denoted σ_0, and the same quantity as that obtained by high-frequency ac measurements. The electrochemical potential gradients of species 1 and 2 are given by

$$\frac{1}{z_1 F}\frac{d\bar{\mu}_2}{dz} = \frac{1}{z_2 F}\frac{d\bar{\mu}_2}{dz} = \frac{d\varphi}{dz}, \tag{3.14}$$

and since $d\varphi/dz$ is constant with z, the first two expressions can be identified with the measured probe voltage differences, divided by the probe spacing, Δz. Thus

$$\Delta V_1 = \Delta V_2 = -\Delta z I_1/\sigma_0 = X \quad \text{(in Fig. 2)}. \tag{3.15}$$

At later times the motion of species 2 becomes blocked since it is unable to enter or leave the ends of the bar and eventually

$J_2 = 0$ everywhere. Eliminating $d\bar{\mu}_2/dz$ between the flux equations one obtains

$$I_1 = z_1 F J_1$$

$$= -\frac{1}{z_1 F}\frac{d\bar{\mu}_1}{dz}\{\sigma_{11} + \sigma_{12}^2/\sigma_{22}\}. \quad (3.16)$$

The term in brackets is the partial conductivity of species 1, denoted σ_1' by Wagner (*17*). Now gradients of composition occur along the sample and σ_{ij} are in general themselves functions of composition. In order to derive useful relations we impose the restriction that the range of composition encountered along the bar specimen be small enough for σ_{ij} values to be taken as constants. As will be seen in Section 5 this is quite readily achievable experimentally. We can thus write

$$\Delta V_1 = -\Delta z I_1 \sigma_{22}/(\sigma_{11}\sigma_{22} - \sigma_{12}^2)$$

$$= Y \quad \text{(in Fig. 2)}. \quad (3.17)$$

Similarly, for the blocked species (species 2), one obtains

$$\Delta V_2 = +\Delta z I_1 \sigma_{12}/(\sigma_{11}\sigma_{22} - \sigma_{12}^2)$$

$$= Z \quad \text{(in Fig. 2)}. \quad (3.18)$$

In the case of zero cross coefficients ΔV_2 returns to zero. Rewriting (3.16):

$$d\bar{\mu}_1/dz = -I_1 F z_1 \sigma_{11}/(\sigma_{11}\sigma_{22} - \sigma_{12}^2). \quad (3.19)$$

This must contain a field gradient term which will be reduced by $z_1 F I_1/\sigma_0$ when at t_1, the current I is switched off. Thus immediately after switching off,

$$d\bar{\mu}_1/dz = -I_1 F z_1 \left\{\frac{\sigma_{11}}{(\sigma_{11}\sigma_{22} - \sigma_{12}^2)} - \frac{1}{\sigma_0}\right\}. \quad (3.20)$$

Hence ΔV_1 falls by the same increment X as that at the initial current switch-on. ΔV_2 does the same (Fig. 1). Finally at infinite time after switching off the bar returns to its equilibrium starting condition. Note that there will have been no change in bulk composition.

Simple algebra gives the following relations for the σ_{ij} values as a function of the experimental quantities X, Y, and Z:

$$\sigma_{11} = \frac{Z^2(X-Y)}{XY(Y-Z)^2} - \frac{1}{Y}; \quad (3.21)$$

$$\sigma_{22} = \frac{Y(X-Y)}{X(Y-Z)^2}, \quad (3.22)$$

$$\sigma_{12} = -\frac{Z(X-Y)}{X(Y-Z)^2}, \quad (3.23)$$

Similarly for the transport numbers:

$$t_1 = (X-Z)/(Y-Z); \quad (3.24)$$

$$t_2 = -(X-Y)/(Y-Z). \quad (3.25)$$

(b) Voltage Probe Behaviour between the Initial and Steady-State Times

The Controlling Transport Process

As seen above it is possible to explain the probe voltages under certain specific conditions just using the flux equations and simple statements about individual fluxes or chemical potential gradients. In the general case, however, it is necessary to solve for the local field $d\varphi/dz$ as a function of the concentrations c_i of the species present. This normally has to be done numerically, and algorithms have been derived, for example by Sandifer and Buck (*23*). Such numerical solutions show, however, that when the concentration of mobile charged species is high, a condition of local charge neutrality holds everywhere except, typically, within about 10^3 Å of the interface. Transport within space charge regions has been discussed thoroughly by Fromhold (*24*). In the present work samples of millimeter dimensions are considered, and it is thus possible to simplify the problem greatly and obtain accurate analytical solutions for the transport

process by making the assumption that local charge neutrality holds everywhere, provided one does not attempt to calculate the field and concentrations of species in space charge regions. In four-point conductivity experiments this is not required, since all that has to be known about the interface between the sample bar and its current contacts is the current density and the species involved. Space charges must also exist at the interfaces between the bar and the voltage probes. However, there is no net flux perpendicular to the z-direction, so chemical equilibrium is maintained across these interfaces and Eqs. (2.4)–(2.7) remain valid.

Ambipolar Diffusion

The condition of local charge neutrality implies that a current of one charged species must be counterbalanced by an opposite current of another species. This coupled motion is described by a single "ambipolar" or "chemical" diffusion coefficient $\tilde{D}$, defined by

$$\tilde{D} = -\frac{J_1}{dc_1/dz} = -\frac{J_2}{dc_2/dz}. \quad (3.26)$$

For a pure diffusion process, therefore, $z_1 J_1 + z_2 J_2 = 0$. Combining this with the flux equations and eliminating $d\varphi/dz$ one obtains

$$J_1 z_1 = -J_2 z_2 = -\frac{(\sigma_{11}\sigma_{22} - \sigma_{12}^2)}{F^2 \sigma_0} \cdot \left\{ \frac{1}{z_1}\frac{d\mu_1}{dz} - \frac{1}{z_2}\frac{d\mu_2}{dz} \right\} \quad (3.27)$$

It is now necessary to relate $d\mu_i/dz$ to dc_i/dz in order that (3.27) can be written in the form of Fick's first law.

To keep the treatment valid for cases where the components are thermodynamically nonideal it is necessary to consider the chemical potential of each component to be affected not only by its own concentration but by those of other components also. This was recently pointed out by Heyne (*25*). Thus for the case under consideration one must write

$$\frac{d\mu_1}{dz} = \left(\frac{\partial \mu_1}{\partial c_1}\right)_{c_2,c_3} \cdot \frac{dc_1}{dz} + \left(\frac{\partial \mu_1}{\partial c_2}\right)_{c_1,c_3} \cdot \frac{dc_2}{dz} + \left(\frac{\partial \mu_1}{\partial c_3}\right)_{c_1,c_2} \cdot \frac{dc_3}{dz} \quad (3.28)$$

and similarly for the other components. The third term vanishes since c_3 is a constant. Furthermore because of local charge neutrality

$$z_1\, dc_1/dz + z_2\, dc_2/dz = 0, \quad (3.29)$$

and Eq. (3.28) becomes

$$\frac{d\mu_1}{dz} = \frac{dc_1}{dz}\left\{ \left(\frac{\partial \mu_1}{\partial c_1}\right)_{c_2,c_3} - \frac{z_1}{z_2}\left(\frac{\partial \mu_1}{\partial c_2}\right)_{c_1,c_3} \right\}.$$

Putting $dc_2 = -z_1\, dc_1/z_2$ in the second term,

$$\frac{d\mu_1}{dz} = \frac{dc_1}{dz}\left\{ \left(\frac{\partial \mu_1}{\partial c_1}\right)_{c_2,c_3} + \left(\frac{\partial \mu_1}{\partial c_1}\right)_{c_1,c_3} \right\}. \quad (3.30)$$

The first partial differential in brackets thus refers to the contribution to $d\mu_1$ from changes in c_1 and the second to the contribution from changes in c_2. *Because* of the local charge neutrality condition, therefore, it is possible to replace the brackets by the complete differential $d\mu_1/de_1$ and thence to replace this by the usual expression involving activities:

$$\frac{d\mu_1}{dz} = \frac{dc_1}{dz} \cdot \frac{RT}{c_1}\frac{d \ln a_1}{d \ln c_1}. \quad (3.31)$$

We have dealt with this section in detail so as to show that the final thermodynamic expression $d \ln a_1/d \ln c_1$ henceforth shortened to w_1, can in fact contain any thermodynamic dependence of μ_1 on c_2, c_3 and as such is quite general. Equation (3.27) can now be rewritten

$$J_1 z_1 = -J_2 z_2 = -\frac{RT(\sigma_{11}\sigma_{22} - \sigma_{12}^2)}{F^2 \sigma_0} \cdot \left\{ \frac{w_1}{z_1 c_1}\frac{dc_1}{dz} - \frac{w_2}{z_2 c_2}\frac{dc_2}{dz} \right\},$$

leading to

$$J_1 = -\frac{(\sigma_{11}\sigma_{22}-\sigma_{12}^2)}{\sigma_0} \cdot \frac{RT}{F^2}\left\{\frac{w_1}{z_1^2 c_1}+\frac{w_2}{z_2^2 c_2}\right\}\frac{dc_1}{dz},$$

from which the ambipolar diffusion coefficient $\tilde{D}$ can be recognized as

$$\tilde{D} = -\frac{(\sigma_{11}\sigma_{22}-\sigma_{12}^2)}{\sigma_0}\frac{RT}{F}\left\{\frac{w_1}{z_1^2 c_1}+\frac{w_2}{z_2^2 c_2}\right\}. \tag{3.32}$$

This important relation, derived by Wagner and Kimball, shows how $\tilde{D}$ is related to the conductivity terms and a thermodynamic factor. It will be shown next that, like the conductivities, this thermodynamic quantity in brackets is also experimentally measurable. We will abbreviate it by W as suggested by Weppner and Huggins (*7*).

When the sample is in equilibrium it was shown that an open-circuit cell voltage E could be measured, given by

$$E = -(z_2\mu_1 - z_1\mu_2)/F. \tag{3.33}$$

Here we include the z_i terms for generality. As the composition of the sample can be varied by coulometric titration it is possible to measure the change in cell emf with composition, say with c_1. Thus one obtains

$$\frac{dE}{dc_1} = -\frac{1}{F}\left\{z_2\frac{d\mu_1}{dc_1} - z_1\frac{d\mu_2}{dc_1}\right\}.$$

With (3.29)–(3.32) this becomes

$$\frac{dE}{dc_1} = -\frac{z_2 z_1^2 RT}{F}\left\{\frac{w_1}{c_1 z_1^2}+\frac{w_2}{c_2 z_2^2}\right\}. \tag{3.34}$$

Hence Eq. (3.32) can be replaced by

$$\tilde{D} = \frac{(\sigma_{11}\sigma_{22}-\sigma_{12}^2)}{z_2 z_1^2 \sigma_0}\frac{dE}{dc_1}.$$

Alternatively in terms of the stoichiometric coefficient x of species 1,

$$\tilde{D} = \frac{(\sigma_{11}\sigma_{22}-\sigma_{12}^2)}{z_2 z_1^2 \sigma_0}\frac{M}{\rho}\frac{dE}{dx}, \tag{3.35}$$

where M is the crystal weight and ρ the density of the solid. It is therefore possible to calculate $\tilde{D}$ from experimentally measurable quantities. In the next section it will be seen that $\tilde{D}$ can also be calculated from the time constant of the time-dependent probe voltage variations, thus making possible an experimental test of self-consistency of the theory.

Probe Voltage "Transients"

It is necessary to solve the diffusion equation

$$dc_1/dt = -dJ_1/dz, \tag{3.36}$$

where J_1 is given by

$$J_1 = -\tilde{D}\frac{dc_1}{dz} + I_1\frac{(\sigma_{11}+\sigma_{12})}{F z_1 \sigma_0}. \tag{3.37}$$

The first term is the contribution from diffusion, while the second represents the external current of species 1. Provided σ_{ij} values are not z-dependent the second term is a constant and only affects the boundary conditions. Assuming also $\tilde{D}$ (and hence w_1 and w_2) is independent of z then a general solution to the equation is given by (*26*)

$$c_1 = \sum_{m=1}^{\infty}(A_m \sin \lambda_m z + B_m \cos \lambda_m z) \cdot \exp(-\lambda_m^2 D t).$$

Yokota (*16*) solved this for the case where $\sigma_{12} = 0$. In the present work we have retained the cross coefficients and obtain by analogy with Yokota's treatment the following: Switching on current I_1 at $t = 0$,

$$c_1 = c_1^0 - \frac{F I_1 L(\sigma_{22}+\sigma_{12})}{z_1(\sigma_{11}\sigma_{22}-\sigma_{12}^2)RTW} \cdot \left\{\frac{z}{L}-\frac{1}{2}+\Phi\left[\frac{z}{L},\frac{t}{\tau}\right]\right\}, \tag{3.38}$$

where c_1^0 is the initial value of c_1, L is the bar length, and the function Φ is given by

$$\Phi\left[\frac{z}{L},\frac{t}{\tau}\right]=\frac{4}{\pi^2}\sum_{m=0}^{\infty}\frac{1}{(2m+1)^2}\cdot\exp\left[-(2m+1)^2\frac{t}{\tau}\right]\cos\left[(2m+1)\frac{\pi z}{L}\right]. \tag{3.39}$$

τ is given by

$$\tau=L^2/\pi^2\tilde{D}. \tag{3.40}$$

Similarly, on switching off current I_1, after the steady state has been reached,

$$c_1=c_1^0+\frac{FI_1L(\sigma_{22}+\sigma_{12})}{z_1(\sigma_{11}\sigma_{22}-\sigma_{12}^2)RTW}\cdot\Phi\left[\frac{z}{L},\frac{t}{\tau}\right]. \tag{3.41}$$

It is now necessary to convert the concentration changes back into electrochemical potential variations to which the observed probe voltages are related. First one can equate the diffusion and flux equation expressions for the flux of species 1:

$$J_1=-\tilde{D}\frac{dc_1}{dz}+\frac{I_1(\sigma_{11}+\sigma_{12})}{Fz_1\sigma_0}=-\frac{\sigma_{11}}{z_1^2F^2}\frac{d\bar{\mu}_1}{dz}-\frac{\sigma_{12}}{z_1z_2F^2}\frac{d\bar{\mu}_2}{dz}. \tag{3.42}$$

Similarly for species 2:

$$J_2=-\tilde{D}\frac{dc_2}{dz}+\frac{I_1(\sigma_{22}+\sigma_{12})}{Fz_2\sigma_0}=-\frac{\sigma_{22}}{z_2^2F^2}\frac{d\bar{\mu}_2}{dz}-\frac{\sigma_{12}}{z_1z_2F^2}\frac{d\bar{\mu}_1}{dz}. \tag{3.43}$$

Eliminating $d\bar{\mu}_2/dz$ from Eqs. (3.42) and (3.43) and replacing $\tilde{D}$ by the right-hand side of Eq. (3.32), one obtains

$$\frac{d\bar{\mu}_1}{dz}=RTWz_1^2\frac{dc_1}{dz}\frac{(\sigma_{22}+\sigma_{12})}{\sigma_0}-\frac{I_1z_1F}{\sigma_0}. \tag{3.44}$$

The two voltage probes are at $z=z'$ and $z=z''$; thus

$$\bar{\mu}_{1(z'')}-\bar{\mu}_{1(z')}=\int_{z'}^{z''}\frac{d\bar{\mu}_1}{dz}dz=RTWz_1^2\frac{(\sigma_{22}+\sigma_{12})}{\sigma_0}\cdot\int_{z'}^{z''}\frac{dc_1}{dz}dz-\frac{(z''-z')I_1z_1F}{\sigma_0}. \tag{3.45}$$

Combining Eqs. (3.45) and (3.38):

$$\Delta\bar{\mu}_1=\Delta V_1z_1F=-\frac{z_1(\sigma_{22}+\sigma_{12})^2FI_1L}{\sigma_0(\sigma_{11}\sigma_{22}-\sigma_{12}^2)}\cdot\left\{\frac{z''-z'}{L}+\Phi\left[\frac{z''}{L},\frac{t}{\tau}\right]-\Phi\left[\frac{z'}{L},\frac{t}{\tau}\right]\right\}-\frac{I_1z_1F(z''-z')}{\sigma_0}. \tag{3.46}$$

Corresponding expressions can be obtained for switching off the current and for species 2. If the probes are disposed symmetrically on either side of the center of the bar, distance Δz apart, then $z''=L-z'$. Noting that $\Phi[z/L,t/\tau]=-\Phi[(L-z)/L,t/\tau]$ the following relations result for the probe voltages:

Switching on I_1:

$$\Delta V_1=-\frac{I_1\sigma_{22}\Delta z}{(\sigma_{11}\sigma_{22}-\sigma_{12}^2)}+\frac{2I_1L(\sigma_{22}+\sigma_{12})^2}{\sigma_0(\sigma_{11}\sigma_{22}-\sigma_{12}^2)}\cdot\Phi\left[\frac{L-\Delta z}{2L},\frac{t}{\tau}\right], \tag{3.47}$$

$$\Delta V_2=\frac{I_1\sigma_{12}\Delta z}{(\sigma_{11}\sigma_{22}-\sigma_{12}^2)}-\frac{2I_1L(\sigma_{22}+\sigma_{12})(\sigma_{11}+\sigma_{12})}{\sigma_0(\sigma_{11}\sigma_{22}-\sigma_{12}^2)}\cdot\Phi\left[\frac{L-\Delta z}{2L},\frac{t}{\tau}\right]. \tag{3.48}$$

Switching off I_1:

$$\Delta V_1 = -\frac{I_1 2L(\sigma_{22}+\sigma_{12})^2}{\sigma_0(\sigma_{11}\sigma_{22}-\sigma_{12}^2)}\Phi\left[\frac{L-\Delta z}{2L}, \frac{t}{\tau}\right], \tag{3.49}$$

$$\Delta V_2 = +\frac{I_1 2L(\sigma_{22}+\sigma_{12})(\sigma_{11}+\sigma_{12})}{\sigma_{11}\sigma_{22}+\sigma_{12}^2} \cdot \Phi\left[\frac{L-\Delta z}{2L}, \frac{t}{\tau}\right]. \tag{3.50}$$

At $t=0$, $\Phi[(L-\Delta z)/2L, 0]=\Delta z/2$, and (3.47) and (3.48) reduce to Eq. (3.15). At $t=\infty$, $\Phi[(L-\Delta z)/2L, \infty]=0$, giving Eqs. (3.17) and (3.18). When $\sigma_{12}=0$ the expressions reduce to those previously reported (*4, 16*). All transients thus have the same characteristic time τ which can be obtained experimentally, noting that the function Φ can be approximated by

$$\Phi\left[\frac{L-\Delta z}{2L}, \frac{t}{\tau}\right] \sim \frac{4}{\pi^2}\exp\left(-\frac{t}{\tau}\right) \cdot \cos\frac{\pi(L-\Delta z)}{2L} \tag{3.51}$$

for $t/\tau > 0.5$ (*16*).

Within this limit the behavior of both sets of probes on switching on and off can be described by

$$|\Delta V_t - \Delta V_\infty| = \alpha \exp[-t/\tau], \tag{3.52}$$

where α is a constant for a particular probe geometry. Thus writing V for $|\Delta V_t - \Delta V_\infty|$ one obtains

$$\ln V = \text{const} - t/\tau. \tag{3.53}$$

τ can thus be obtained from the slope of a graph of $\ln V$ against t (*4*). Using a least-squares regression it is normal to minimize the quantity $(\delta \ln V)^2$. However, $\delta \ln V = \delta V/V$ and the experimental errors in V are expected to be largely independent of V. We therefore use a weighted regression which minimizes the quantity $(\delta V \ln V)^2$. τ is consequently given by

$$\tau = \frac{(\Sigma Vt)^2 - \Sigma V \cdot \Sigma(Vt)^2}{\Sigma V \cdot \Sigma(Vt \ln V) - \Sigma Vt \Sigma V \ln V}. \tag{3.54}$$

To comply with the restriction $t/\tau > 0.5$ one makes use of the following relation derived from any one of Eqs. (3.47)–(3.50):

$$\frac{\Delta V_{t(\text{lim})} - \Delta V_\infty}{\Delta V_0 - \Delta V_\infty} = 2L\Phi\left[\frac{L+\Delta z}{L}, 0.5\right] = \text{lim}. \tag{3.55}$$

Only results for which $(\Delta V_t - \Delta V_\infty)/(\Delta V_0 - \Delta V_\infty) < \text{lim}$ are used in the summations of Eq. (3.54).

4. Experimental Techniques

In Sections 2 and 3 the advantage of four-point over two-point conductivity measurements was shown to be the elimination of errors due to resistance at the current contacts as well as those due to deviations from local charge neutrality in these regions. In the case of ionic currents these contacts are formed between a mixed conductor and an electrolyte. The origins of contact resistance between ionic conductors are as yet poorly understood, and since in general the two crystal structures involved are unrelated to each other, it is not an easy subject to treat theoretically, even when single crystals are involved. However, it is obvious that the two surfaces must be free from nonconducting contaminants and in as intimate contact with one another as possible. If one of the phases is relatively soft this can be achieved by application of small-to-moderate pressures. This is the case with most silver and copper conductors that have been studied, and it is not coincidence that these materials have been the subject of the majority of studies involving four-point measurements. Interfaces between $Cu_xMo_6S_8$ or $Cu_{2-x}S$ and the

copper ion-conducting electrolyte 1,4-dimethyl-1,4-diazabicyclo(2,2,2)octane dibromide–CuBr (subsequently abbreviated by T) were made, for example, simply by pressing together polycrystalline pellets and found to exhibit very little contact resistance (*14, 27*). On the other hand, in a study of $K_{1+x}Fe_{11}O_{17}$, a hard polycrystalline ceramic which had to be connected to the hard electrolyte K-β-alumina, dry pressed contacts were found to be unsatisfactory even if the surfaces had been polished, and use had to be made of a trace of molten KNO_3 to promote ionic contact (*4*). All good lithium and sodium electrolytes so far developed are similarly hard materials, and the same difficulty is expected unless the sample itself is soft. This is the case, for example, with transition metal dichalcogenides and satisfactory ionic contacts between the phases Li_xTiS_2/Li_4SO_4–Li_3PO_4 (*27*) have been made. Recently developed thin polymer electrolytes (*28*) for all the alkali metals promise to be of great value when sandwiched between hard materials, for temperatures below 200°C.

Ionic Voltage Probes

Here the interface requirements are much less severe since only very small currents are allowed to flow. Because of the requirement of forming fairly sharp points, hard electrolytes are to be preferred here. The reference material can be pressed against the electrolyte, e.g., Li_3PO_4–Li_4SiO_4/Li_5FeO_8, Cu/T although in the second case better voltage stability was obtained when the electrolyte was first coated with vacuum-evaporated copper. In the special case of $KGa_{11}O_{17}/K_{1.6}Ga_{5.5}Fe_{5.5}O_{17}$ it was possible to form the interface by a hot pressing technique (*4*). The main contribution to the probe resistances comes from the point contact with the sample. Nevertheless, probably because of the very high local pressures at the probe tip, probe impedances have generally been low enough for the use of a conventional 10^{10}-Ω input impedance digital voltmeter even in the case of contacts between two hard materials. The inert metal/mixed-conductor contacts can usually be made simply by pressing a metal foil into the sample, though previous vacuum deposition of gold is to be preferred.

Experimental Jigs

The main practical difficulty in using four-point ionic techniques arises from the need to make numerous contacts all under pressure and that will be stable at moderate temperatures, and not affected by temperature changes. This difficulty is increased in studying mixed conductors by the need to employ bar samples of short lengths to minimize the time taken between switching on a current and reaching the steady state. In practice this time is about 8τ and from Eq. (3.40) is proportional to the square of the bar length. For $D = 1\times10^{-6}$ to 1×10^{-5}, typical values for good SSEs, a bar of length of 5 mm requires times between 6 and 60 hr.

The arrangement used by the present authors is shown in Fig. 3. A stainless-steel G-clamp holds together the sample, electrolyte slices, reservoirs, and electronic contacts, using alumina spacers as insulators where necessary. A nut is screwed onto the threaded part of the G-clamp to keep the jaws open during assembly. When the

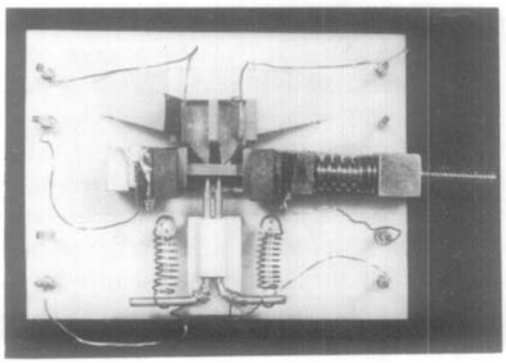

FIG. 3. Experimental jig for carrying out six-point or eight-point conductivity experiments on mixed conductors.

components are in place the nut is removed, leaving the cell clamped by the tungsten compression spring. This assembly is then laid on the alumina baseplate which holds the two sets of voltage probes, the ionic probes being fixed while the electronic probes are sprung by tungsten tension springs. Tungsten has been found satisfactory up to 700 K and the springs can be formed simply by wrapping 0.25- to 0.5-mm-diameter wire around the thread of a small bolt.

To make assembly easier the contacts from the cell are wrapped around a Pt/10% Rh square section contact post using a wire-wrapping tool and these in turn are wire-wrapped to a second set of contacts carried on an alumina baseplate and permanently connected through a horizontal support tube to the outside of the apparatus. The whole assembly sits inside a glass tube in which the atmosphere can be controlled, and which if necessary can be assembled and sealed within a glove manipulator box.

Bar Shape and Probe Positioning

In principle the voltage probes may be placed any distance apart between the current contacts. Although a large spacing produces higher voltages to measure for a given current through the bar, two other factors indicate advantages in having the ratio z/L fairly small (we will assume always that the probes are place symmetrically on either side of the midpoint of the bar side). The first is the shape of the voltage transients. Immediately after the current is switched on or off, composition changes begin to take place from the ends of the bar. Thus probes placed near the current contacts respond rapidly, whereas probes nearer the center show a delay before the voltage changes from the value at switch on/off. It is easier in the second case, therefore, to measure the voltage X (Fig. 2).

The second factor concerns errors due to imperfect current contacts at the ends of the bar. The theory assumes a uniform current density along the bar, but in practice this may not be achieved. In order to investigate the errors produced in the steady-state probe voltages a worst-case model was chosen where the current contacts were restricted to small regions in the corners of the ends of the bar as shown in Fig. 4. The bar was divided into a set of $5\times5\times15$ boxes, and Fick's second law for the diffusion of particles in the boxes was solved numerically with a simple computer program. The currents were simulated by adding particles at a constant rate to the box at one corner and removing the same number at the other corner. After sufficient iterations a time-invariant state was reached. Comparing the concentrations in boxes along the middle of the sides of the bar with those expected for ideal current contacts, and assuming a proportionality between voltage and composition, we calculated the errors involved; they are shown in Fig. 4 for two bars of square cross section but different width/length ratios, as a function of the probe spacing/bar length ratio. Again it can be seen that the errors are significantly reduced for probes close together. As would also be expected the errors fall rapidly with decreasing bar width/bar length ratio. We find therefore that the optimum probe spacing is about one-third of the bar length and that the bar should have as small a cross section as is practicable.

Diffusion coefficients were also calculated from the computer simulations of the transients. Unlike the conductivities they were very insensitive too nonideal current contacts and values for $d/L=0.29$ were within 0.2% of the ideal value in all cases. The assumption was made, of course, that the material was an isotropic conductor. When this is not so, much larger errors can result. The tolerance of this technique to nonuniform current contacts has enabled eight-point experiments to be carried out where both ionic and electronic current contacts are provided at the ends of the bar (*4*).

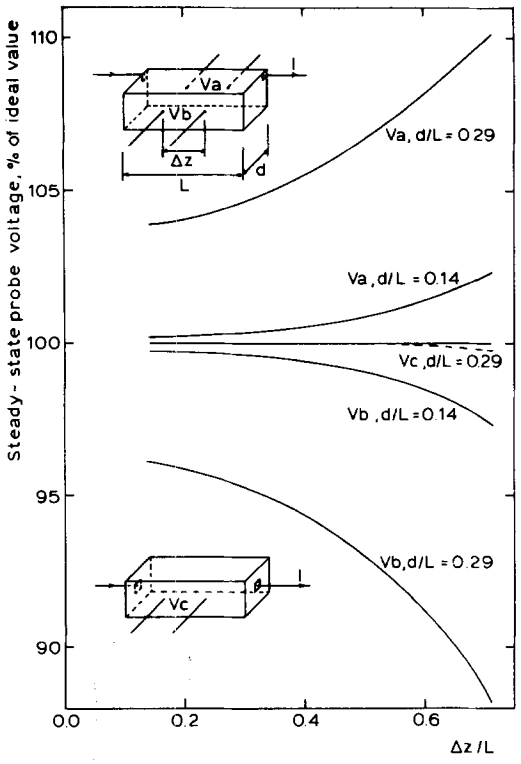

FIG. 4. Errors in steady-state probe voltages when current contacts are not uniform.

5. Experimental Tests of the Theory

Yokota (*16*) showed that the transients observed with $Ag_{1.93}Te$ agreed with values calculated from Eqs. (3.46) to (3.49) with $\sigma_{12} = 0$. Equation (3.35) allows a check of internal consistency to be made, by comparing $\tilde{D}$ calculated from the transients (via τ) with that obtained from the steady-state conductivities σ_{11}, σ_{22} (and σ_{12}) and the slope of the coulometric titration curve. Agreement between these values was within 10% in the case of $Ag_{1.93}Te$. Similar tests for the phase $K_{1+x}Fe_{11}O_{17}$ were also in reasonable agreement with theory, considering the greater experimental difficulties (*4*). This system was of particular interest since the two component conductivities σ'_K and σ'_e were of comparable magnitude and either could be made to dominate depending on the composition. Good agreement was also obtained for the phase $Cu_xMo_6S_8$, which is a metallic conductor (*5*). Miyatani (*9*) investigated the effect of varying the bar length and verified that $\tau \sim L^2$. The theory has thus been quite well verified experimentally.

It is interesting that the cross terms L_{ij} or σ_{ij} have been found to be negligible or at least very small compared to the main term for the species with the lower conductivity for all systems so far studied.

6. Comparison of the Technique with Others

The other most widely used techniques for measuring $\tilde{D}$ in mixed conductors involve the imposition of voltages, constant currents, or current pulses across an interface between the sample and a suitable electrolyte. With solid electrolytes difficulties result because of the requirement of uniform contact and well defined interfacial area.

The main practical advantage of the polarization method is that it relaxes this requirement considerably, allowing completely solid state arrangements to be used and hence wider temperature and metal activity ranges can often be covered. Because of the rather longer diffusion path, however, the method is restricted in practice to materials with high diffusion coefficients ($\tilde{D} > 5 \times 10^{-7}$ cm^2·sec^{-1}), whereas pulse and galvanostatic methods allow much smaller diffusion coefficients to be measured, although account must be taken of the effects of double-layer charging at relatively short times. Also, in the galvanostatic and pulse methods it is only possible to derive σ'_i from $\tilde{D}$ and the thermodynamic factor when $\sigma'_e \gg \sigma'_i$. An extension to the galvanostatic determination of diffusion coefficients has been developed by Weppner and Huggins (*7*), in which the charge passed during diffusion experiments serves also to change the composition of the sample slightly so that an alternation of such experiments with equil-

ibration periods allows determination of $\tilde{D}$ as a function of stoichiometry. The method has accordingly been called the galvanostatic intermittent titration technique, and has been used for systems such as $Li_{3-x}Sb$ (*29*). The composition can also be changed by coulometric titration in the case of the polarization method, but this is only possible when there is no material in direct contact with the bar to maintain a known activity of metal (unlike, for example, in the Hebb–Wagner experiment) and the technique has been criticized on this account (*7*). However, when both ionic and electronic voltage probes are present the metal activity in the bar can be simply measured from the voltage difference between the two sorts of probes and this criticism is no longer valid.

The choice of method to be used for a particular mixed conductor depends mainly on whether the most convenient electrolyte is liquid or solid, whether it is practical to machine a bar-shaped sample, and how large the chemical diffusion coefficient is expected to be.

Automatic Control of Experiments

Because of the time-consuming nature of the chemical diffusion coefficient determinations and the coulometric titrations some sort of automatic control is highly desirable. This need only be a relatively simple data logger or chart recorder to record variation of voltages with time, but with the recent introduction of cheap microcomputers complete automatic control of sequences of experiments has become possible at reasonable cost. This will form the subject of another paper.

Appendix: List of Symbols

a_i	Activity of species i
B_{ij}	Absolute mobility of i with respect to flows of j
c_i	Concentration of i
$\tilde{D}$	Chemical (or ambipolar) diffusion coefficient
e	Electron
E	Cell emf
F	The Faraday
I_i	Current density of species i
i, j	Subscripts for generalized components
J_i	Molar flux of i
L	Length of bar specimen
L_{ij}	Phenomenological coefficient in flux equations
M	Formula weight of the mixed conductor
R	Molar gas constant
t	Time
t_i	Transport number of species i
T	Absolute temperature
ΔV_i	Voltage difference between probes reversible to i
V	$\lvert\Delta V_t - \Delta V_\infty\rvert$ for any voltage probes
w_i	Thermodynamic factor for single species i $(d \ln a_i / d \ln c_i)$
W	Overall thermodynamic factor $\sum_i w_i / z_i^2 c_i$
x	Deviation from stoichiometry
X, Y, Z	Voltage differences measured in a four-point experiment
z	Distance coordinate along direction of diffusion
z_i	Number of charges carried by species i
Δz	Voltage probe spacing
μ_i	Chemical potential of species i
$\tilde{\mu}_i$	Electrochemical potential of species i
φ	Electrostatic potential
σ_{ij}	Conductivity coefficient
τ	Characteristic time of voltage probe transients

References

1. B. C. H. STEELE, *in* "Superionic Conductors" (G. D. Mahan and W. L. Roth, Eds.), pp. 47–65, Plenum, New York (1976).
2. M. ARMAND, Thesis, University of Grenoble (1978).
3. M. S. WHITTINGHAM, *Progr. Solid State Chem.* **12**, 1 (1978).
4. G. J. DUDLEY AND B. C. H. STEELE, *J. Solid State Chem.* **21**, 1 (1977).
5. G. J. DUDLEY, K. Y. CHEUNG, AND B. C. H. STEELE, submitted for publication.
6. C. WAGNER, *in* "Proceedings, 7th Meeting C.I.T.C.E., Lindau, 1955," Butterworths, London (1957).
7. W. WEPPNER AND R. A. HUGGINS, *Ann. Rev. Mater. Sci.* **8**, 269 (1978).
8. S. MIYATANI AND Y. SUZUKI, *J. Phys. Soc. Japan* **8**, 680 (1953).
9. S. MIYATANI, *J. Phys. Soc. Japan* **24**, 328 Fig. 6, (1968).
10. S. MIYATANI, *J. Phys. Soc. Japan* **34**, 423 (1973), and papers quoted therein.
11. H. RICKERT, *Z. Phys. Chem. N.F.* **23**, 355 (1960).
12. T. TAKAHASHI AND O. YAMAMOTO, *J. Electrochem. Soc.* **119** 1735 (1972).
13. G. J. DUDLEY AND B. C. H. STEELE, *J. Electrochem. Soc.* **125**, 1994 (1978).
14. G. J. DUDLEY, K. Y. CHEUNG, AND B. C. H. STEELE, submitted for publication.
15. I. YOKOTA, *J. Phys. Soc. Japan* **8**, 595 (1953).
16. I. YOKOTA, *J. Phys. Soc. Japan* **16**, 2213 (1961).
17. C. WAGNER, *Progr. Solid State Chem.* **10**, 3 (1975).
18. J. C. KIMBALL, *Phys. Rev. B* **16**, 785 (1977).
19. G. C. FARRINGTON, *J. Electrochem. Soc.* **123**, 1213 (1976).
20. U. V. ALPEN, M. F. BELL, W. WICHELHAUS, K. Y. CHEUNG, AND G. J. DUDLEY, *Electrochim. Acta* **23**, 1395 (1978).
21. T. OHACHI AND I. TANIGUCHI, *Electrochim. Acta* **22**, 747 (1977).
22. A. T. FROMHOLD, JR., S. R. CORIELL, AND J. KRUGER, *J. Phys. Soc. Japan* **34**, 1452 (1973).
23. J. R. SANDIFER AND R. P. BUCK, *J. Phys. Chem.* **79**, 384 (1975).
24. A. T. FROMHOLD, JR., *in* "Theory of Metal Oxidation," Vol. 1, North-Holland, Amsterdam (1976).
25. L. HEYNE, *in* "Solid Electrolytes" (S. Geller, Ed.), Springer-Verlag, Berlin (1977).
26. J. CRANK, "The Mathematics of Diffusion," 2nd ed., p. 17, Oxford Univ. Press (Clarendon), London.
27. G. J. DUDLEY, unpublished work.
28. M. ARMAND, 2nd International Meeting on Solid Electrolytes, St. Andrews, Scotland, U.K., Sept. 1978.
29. W. WEPPNER AND R. A. HUGGINS, *J. Electrochim. Soc.* **124**, 1569 (1977).